International Journal of Bio-Science and Bio-Technology
Vol.8, No.1 (2016), pp.105-120
http://dx.doi.org/10.14257/ijbsbt.2016.8.1.10

# A Comparative Study on Left and Right Endocardium Segmentation using Gradient Vector Field and Adaptive Diffusion Flow Algorithms

Yabrin Amin[1], Shoaib Amin Banday[2], A.H.Mir[2]

[1]*Deptt. of Electronics and Communication Engineering, ASET, Amity University, Noida, India-201313*
[2]*Deptt. of Electronics and Communication Engineering, NIT Srinagar, J&K India-190006*
[1]*yabrin7483@gmail.com*, [2]*shoaibee.a@gmail.com*, [3]*ahmir@nitsri.net*

***Abstract***

*The cardiac Magnetic Resonance Imaging (MRI) provides high resolution images of the heart without radiation exposure. It is an excellent noninvasive test used by radiologist for proper detection of heart diseases. The manual segmentation of left ventricle in cine short axis MRI sequences takes an ample amount of time as compared to semi-automated segmentation. In Gradient Vector Flow (GVF) model certain barriers hinder the performance such as weak edge detection, high computational time, limited capture range and its ambiguity with other parameters. In this paper segmentation of Endocardium is carried out on multistage MRI frames Using Adaptive Diffusion flow (ADF) model. This deformable model was tested on large scale number of Cardiac MRI images. We replace the smoothening energy term in GVF with active hyper-surface harmonic minimal function in order to avoid possible leakage at weak edges. The use of harmonic maps is adjusted in accordance with image characteristics. We also assimilate infinite Laplace function to move active contours into narrow concave sections. Experimental results and collation with GVF are presented in this paper which reveals several good results based on extraction of endocardium tissue from left and right ventricle, including less computational time, noise robustness and weak edge preserving on Cardiac MR Images.*

**Keywords**: *Endocardium segmentation, Snakes, Magnetic Resonance imaging (MRI), Active contours, Adaptive diffusion flow (ADF), Gradient vector flow (GVF).*

## 1. Introduction

Active contour models [2], or deformable models [3], or snakes, have been found to be effectual implementation for image segmentation, tracking [6-8] and shape recovery [9] etc. Snakes [2] are used in computer vision and image analysis to identify and locate objects. They can also be used to find the outline or describe the shape of an organ in medical imaging by radiologists [1]. The Cardiac Magnetic Resonance Images (MRI) are being processed on deformable models so as to extract the endocardium wall with the help of snake models. Since it is one of the most active and flourishing research in the field of image segmentation [3] so they are categorized as: Point based deformable models, Parametric deformable models [10, 11] and Geometric deformable models. The most widely used deformable models comprise of active contours [2] and active surfaces [3]. The active contours capture a desired section by minimization of energy to certain constraints. The deformable models contains two integral energy forces: The Internal forces are responsible for determining the curve or surface within an image in order to keep model smooth during deformation, while as External forces are computed from image so that the snakes will interlock itself to the object boundary as per the feature of interest.

ISSN: 2233-7849 IJBSBT

This paper emphasizes more on the internal and external forces of Gradient Vector Flow (GVF) and Adaptive Diffusion flow (ADF) which has been thoroughly studied [10, 11, 14]. Although the most successful and used external forces for GVF has been proposed by Xu and prince [11] which leads to several modified versions of active contour models. But the researchers found that GVF suffers from several disadvantages including leakage problems at weak edges, ambiguity with other parameters [4, 5] as well as narrow and deep edges convergence [4].

The main aim of this paper is to segment Endocardium layer from left and right ventricle for proper diagnosis, associated with manual segmentation and compares the processing speed of GVF and ADF active contours with computational time. Also, is an extension to Modified Vector Flow (MGVF) algorithm [1]

## 2. Background

### 2.1. Gradient Vector Field Active Contour Model (GVF Snakes)

The conventional active contours are limited to imperfect convergence and capture extent to boundary cavities. GVF was introduced by Xu and Prince [11] as an improved external force for deformable models to overcome these two key difficulties of snakes. GVF force field is stated as a vector field *V(x,y)={u(x,y),v(x,y)}* that is responsible for the energy minimization functional given as:

$$E = \{\iint \mu( u_y^2 + u_x^2 + v_y^2 + v_x^2) + (|\nabla f^2| \, |V\text{-}\nabla f^2|)\}\text{dydx} \qquad (1)$$

The above equation comprises of both the smoothness and edge energy. $f$ in the second term is the edge map of the input image I(x,y). When the Cardiac MRI is loaded as an input image, the edge map is being derived from the image I(x,y) itself. $|\nabla f|$ is large near the edges and almost negligible in uniform regions. μ is basically used for the balancing of the above equation and is referred a positive weight. This equalization parameter, sets according to the amount of noise present in Cardiac MR Images. If more noise is present, there will be an increase in μ factor.

However there are various noise removal methods like, linear filtering, adaptive filtering, median filtering, morphological filtering & anisotropic diffusion that can be used for preserving edges as well as other high frequency parts of an image I(x,y) [12,13]. The short axis Cardiac MR Images used in this paper undergoes Gaussian smoothing noise reduction technique for eliminating noise factor. By minimizing Eq. 1, GVF field can be solved by using Euler's Lagrange equation.

$$\left[\mu\nabla^2 V - \{(V - \nabla f)\left(f_y^2 + f_x^2\right)\}\right] = 0 \qquad (2)$$

Using Dynamic approach in Eq. 2 and substituting V as a function of x, y and t can be re-written as:

$$\frac{dv}{dt} = \{\mu\nabla^2 u - (u - f_x)\left(f_y^2 + f_x^2\right)\} = 0$$

$$\frac{dv}{dt} = \{\mu\nabla^2 v - \left(v - f_y\right)\left(f_y^2 + f_x^2\right)\} = 0 \qquad (3)$$

Where $\nabla^2$ in the above two terms is called as Laplacian operator. The second term in both the equations reduces to Zero as the gradient of *f(x,y)* is zero. The GVF field is obtained by above two equations with V(x,y) as an external force.

 

### 2.2. GVF Limitations

GVF has overcome the problem of modelling adequate capture range and capability to capture boundary cavities e.g. U shaped convergence, proposed by Bing Li and Scott T. Acton [5]. Although GVF has been extensively used and enhanced in various upgraded models [12,13,14] but there are some drawbacks, like weak edge leakage, high computational time, noise sensitivity, limited capture range and its ambiguity with other parameters.

### 2.3. Endocardium Segmentation: Survey

Segmentation of cardiovascular medical imaging leads to numerous applications, which can mend the diagnostics of heart maladies. The Manual segmentation of cardiac images by human specialists can be time intensive. For these diagnosis, computerized semiautomatic segmentation of the right and left ventricle in heart short axis MR images is of great attraction and has to deal with many challenges, e.g. extracting the desired tissue boundaries, like those between the endocardium tissue and the centered hemoglobin pool can have low disparity.

Further, strong active external forces may exist where boundaries are not desired. Segmentation or division methods having data taken in account from the image alone do not function properly in such cases and supplementary restraints are important to include as explained in level set-based segmentation method for heart images [16]. There are also other methods based on combining boundary, zone and contour data analysis for the segmentation purpose [17]. These calculations and algorithms require a lot of preparing cases, which can be difficult to get and is a period expending procedure and hence increases the amount of investment which make them costly procedures.

In short-pivot MR heart pictures, the left ventricle generally resembles the appearance of a toroid. Therefore, less complex parametric shape was utilized which don't experience any factual preparing, may address the issues. The chart cuts-based segmentation technique has get to be broad in light of the fact that it considers a generally perfect effective answer for N-dimensional parameters [17, 18]. Despite of its numerous choices, chart cuts are incapable of producing a precise divisions of images with feeble edges. Another novel methodology consolidates deformable models, which do not require plot based training like that of the chart cuts method for the productive endocardium segmentations in heart images. In some automatic approaches the segmentation methods all alone cannot work efficiently so the additional restraints are included. The estimation and maximization methods (EM-style approach) including quantitative calculations shows the poor visualizations of left ventricle [22] as compared to our method. Many algorithms like Gradient vector flow (GVF) [14], Modified Gradient vector flow (MGVF) [1] and Vector flow convolution (VFC) [5] etc. are used in Cardiac MR Images in which irregular edges are encountered.

## 3. Methodology

Adaptive diffusion flow snake model provides a novel external force, which is in accordance with the characteristics of cardiac MR image regions in parametric models implementation for image segmentation. In this section, we adopt a method in order to seek solution to the problems faced by GVF snakes using theoretical and mathematical approach of ADF external forces.

### 3.1. Hyper-surface Harmonic Minimal Functional Analysis

The smoothing energy term in the original GVF is replaced by hyper-surface harmonic minimal functional. The only difference between the two is that, this equation has strong regularizing properties in almost all directions. In order to obtain an improved adaptive diffusion, the areas where intensity is weak discovered and hence pondered upon. Let us consider the image I (x,y) using image function defined by: I (x,y): $(0,w) * (0,h) \rightarrow R^2$. Let f be an edge map of image I (x,y), Ω be an constrained open subset of $R^2$ and $d\Omega$ its boundary. So, the hyper-surface harmonic function is defined as

$$E(v) = \left\{ \iint \frac{1}{p|\nabla f|} \left( \sqrt{1 + |G_\sigma \otimes \nabla v|^2} \right)^{p|\nabla f|} \right\} \qquad (4)$$

where $p|\nabla f|$ is monotonous decreasing function which can range in between 1–2. In our method we choose $p|\nabla f| = \{1 + 1/(1 + |\nabla G_\sigma \otimes f(y)|)\}$, if $|\nabla G_\sigma \otimes f(y)| = 0$, $p|\nabla f| = 2$ which in homogeneous regions is a case of isotropic diffusion.

Also, when $|\nabla G_\sigma \otimes f(y)| = \infty$, $p|\nabla f| = 1$. Therefore, Eq. 4 on the edges would behave like total variant image restoration model [15] where diffusion will only occur in the direction parallel to the boundaries. This proves that the hyper-surface harmonic function yields to smooth vector force field and preserves weak edges.

### 3.2. Infinite Laplace Functional Analysis

Another limitation of GVF is reaching the deep and narrow cavities. As Laplacian operator comprises of directional derivatives, normal and along the tangent. The diffusion with respect to normal direction plays a vital role in GVF model. So, more emphasis is laid on boundary cavities. Vectors are directed downwards rather than disappearing far from cavities, or converging from two face to face directions. As discussed in [11], vector fields using infinite energy Laplacian energy function is used to minimize Lipschitz extension $L^P$, which is explained as:

$$E_\infty v = \int |\nabla G_\sigma \otimes \nabla v|^P \, dx \qquad (5)$$

Substituting $P \to \infty$ in Eq. 5, we get

$$E_\infty v = \int |\nabla G_\sigma \otimes \nabla v|_{L^\infty(\Omega)} \, d\Omega \qquad (6)$$

Therefore the minimization of Eq. 6 is termed as the absolute minimizing Lipschitz interpolate equation.

 

### 3.3. Adaptive Diffusion Flow Snake (ADF)

The conceptual and theoretical foundation of ADF has been already described in above two sections of methodology. Using the following formulation, diffusion framework of ADF can be obtained. The Endocardium segmentation of cardiac MRI is efficiently implemented as compared to the GVF segmentation, due to anisotropic diffusion. The ADF formulation is given as:

$$E(v) = \left[ \left\{ \iint g * \left(-m\, |\nabla G_\sigma \otimes \nabla v\,|_{L^\infty(\Omega)} + (1 - \quad m) \left(\frac{1}{p|\nabla f|}\right) \left(\left(\sqrt{1 + |G_\sigma \otimes \nabla v|^2}\right)^{p|\nabla f|}\right)\right\} d\Omega \right. \\ \left. + \iint \{h\,(|v - f(y)|^2)\}\, d\Omega \right] \qquad (7)$$

where $|G_\sigma \otimes \nabla v|^2 = \Theta$ and m, g, h are the weighting functions. Similarly u can also be obtained from Eq. 7. So, a new external force is implemented over the traditional snake models. As initialization is one of the important parameters for the extraction of endocardium wall in left and right ventricle, choosing suitable values of weighting functions is critical so as to prevent weak edges or boundaries of cardiac MR images. The values of h and g are similar as explained in GGVF [ref], whereas m depends on:

$$\mathrm{m} = \begin{cases} \left(1 - \frac{f^2}{5k^2}\right)^2, & if\ \frac{f^2}{5} \le k^2 \\ 0, & otherwise \end{cases} \qquad (8)$$

In above equation, k preserves the contrast of edges and k = 1.482 $*\, mean\ value\ [E\{||\nabla f| - mean\ value * (|\nabla f|)|\}]$[20].

### 3.4. Flowchart of Algorithm

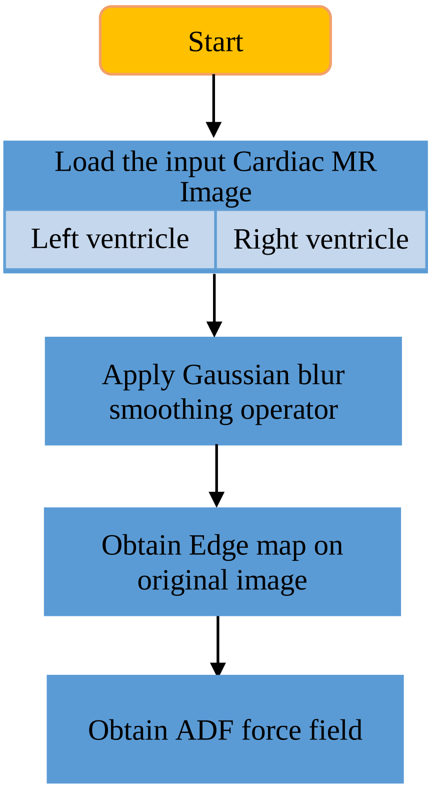

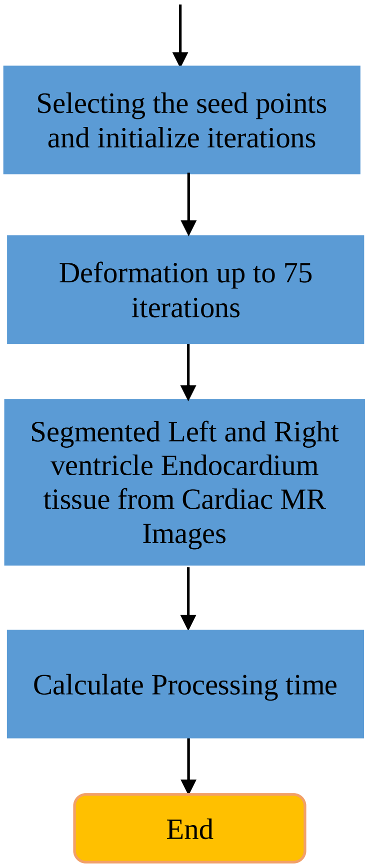


## 4. Results and Analysis

In this section, ADF snake is applied on the real noisy Cardiac M R image in order to demonstrate the improved and better results with some desirable properties. We describe comparative Endocardium segmentation results of ADF and GVF snakes with CPU processing time (in seconds). The values of $\alpha, \beta, \sigma$ and $\tau$ are kept as 0.5, 0.5, 0.9 and 1 respectively.

An open access database for Cardiac M R Images is provided by Auckland (New Zealand) Medical Research Centre. The experimental results of ADF active contours are finally obtained and locked in both the ventricles as shown in Fig. 3. Further the semi-automatic based segmentation (i.e. ADF snake model) of the left and right ventricle is analyzed with manual segmentation. The manual segmentation of cardiac MRI is done by Dr. M. A. Zargar at Ministry of Health, Maldives. The general demographics of normal patient were analyzed before performing the semiautomatic ADF algorithm on cardiac MRI.

### 4.1. Seed Points Initialization and Curve Evolution

The initialization is done with the help of the seed points and the other parameters are adjusted accordingly on any cardiac M R image among different slices of short axis as shown in Fig. 1. The number of seed points taken for the segmentation of left and right ventricle are 22 and 30 respectively.


**Figure 1. One Cardiac Cycle MRI Views at Different Slices along Short Axis**

Sensitivity parameter *k* is responsible for edge preservation, k should be small if the edges are leaky and vice versa. We kept on substituting different values of k and found the best possible resulting outcomes on interval [0.04, 0.2] for the loaded cardiac MR images. The red dashed lines represent the initiation and evolution of curve as shown in Fig. 2.

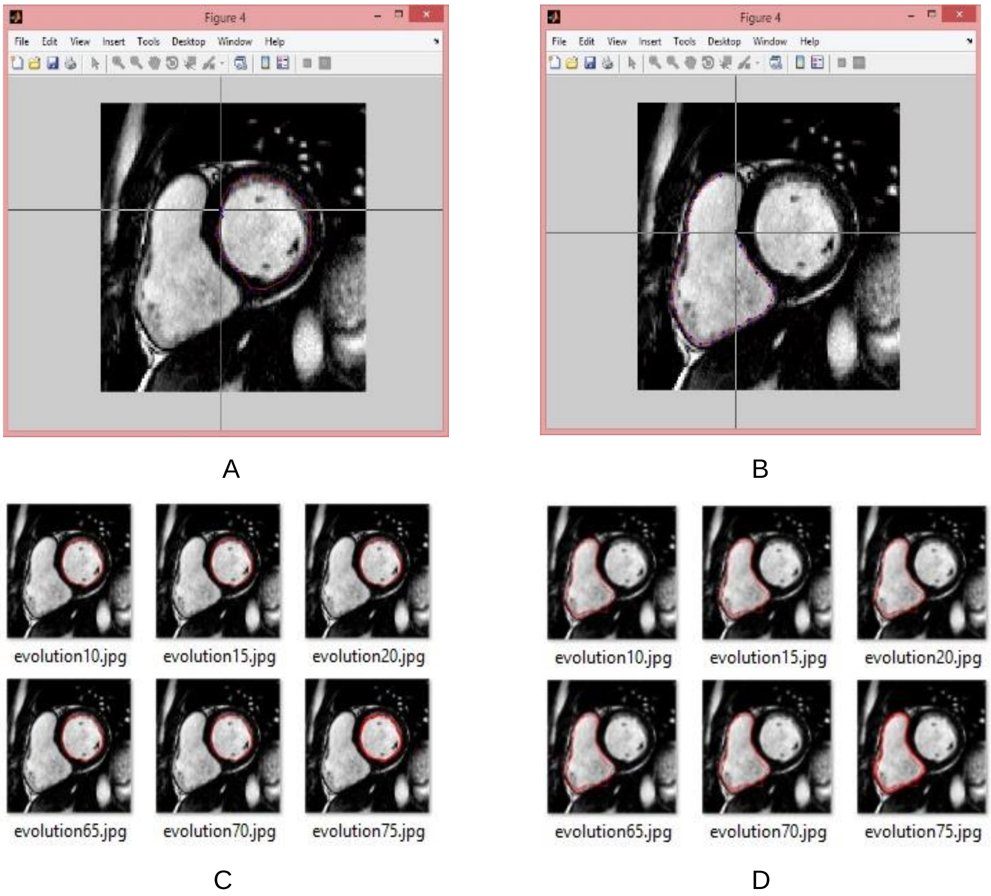


**Figure 2. (A) Initiating Seed Points on LV (B) Initiating Seed Points on RV (C) the Evolution of Curve on Left Ventricle (D) Evolution of Curve on Right Ventricle**

### 4.2. Segmented ADF Cardiac MRI Outputs

The step by step segmented Endocardium tissue of left and right ventricle from Cardiac MRI is undergoing the process of initialization, curve evolution and eventual result as shown in the below given figures. The red outline shows the extracted results using ADF algorithm as shown in Fig. 6.

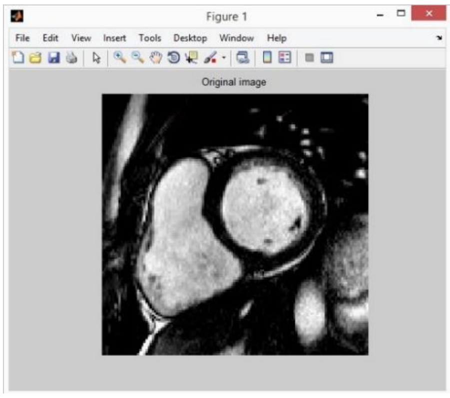


A

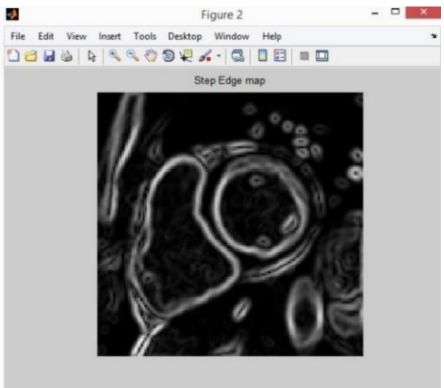


B

**Figure 3. (A) Cardiac MR Input Image. (B) Applying Smoothing Gaussian Filter and Obtaining Edge Map**

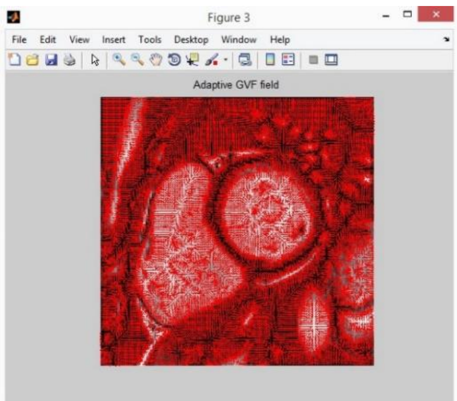


**Figure 4. ADF Force Field**

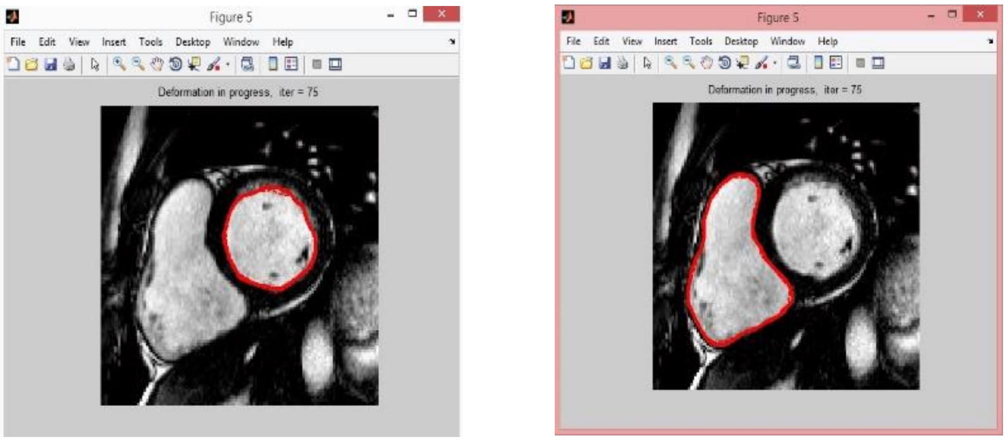


A B

**Figure 5. Deformation in Process. (A) Left Ventricle (LV). (B) Right Ventricle (RV)**

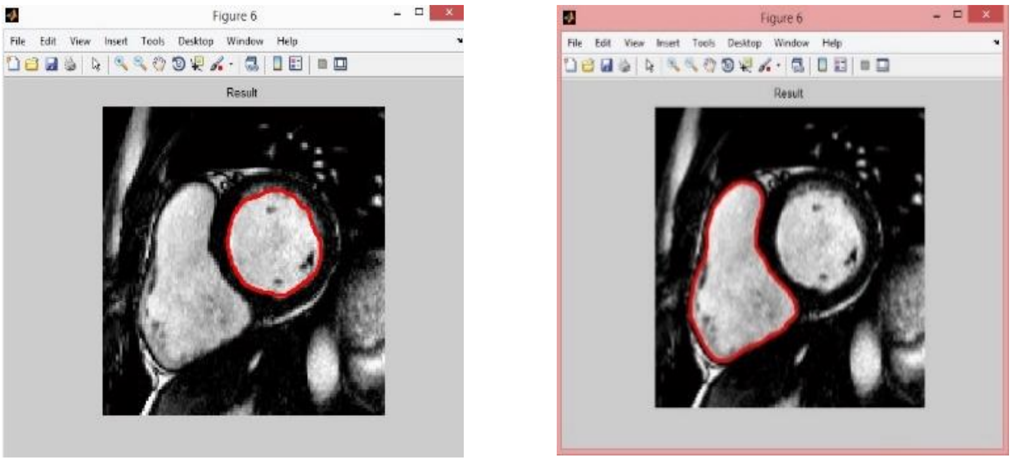


A B

**Figure 6. Final Results of Endocardium Tissue Extraction Obtained in 75 Iterations. (A) Automated Segmented LV. (B) Automated Segmented RV**

### 4.3. Comparative Results of ADF with GVF

According to the analysis in section III, the experiment is carried out to solve the issue of leakage around weak edges using ADF active contour snake model. Fig 8 shows the segmented Cardiac MR Image of right and left ventricle. The value of μ for the GVF snake model is taken as 1.05 and the edge map $f(x, y) = G_\sigma(x, y) \otimes I(x, y)$ is obtained after anisotropic diffusion.

It is observed that the GVF snakes are driven towards the strong contours instead of weak so, the GVF model fails to extract the true boundaries of cardiac MR Images. Even though the GVF model is well known for the smoothing of image, it does not prevent the edges or the boundary leakage as shown in Fig. 7(b)

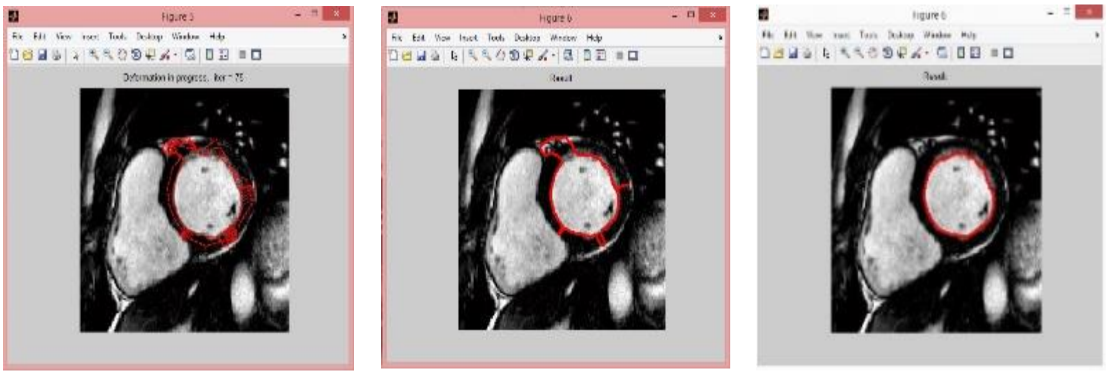

A B C

**Figure 7. ADF and GVF Results based on Left Ventricle. (A) Initial Curves of GVF. (B) Result of GVF Model with $\mu = 1.05$ (C) Result of ADF with $\sigma = 0.9$ and $k = 0.04$**

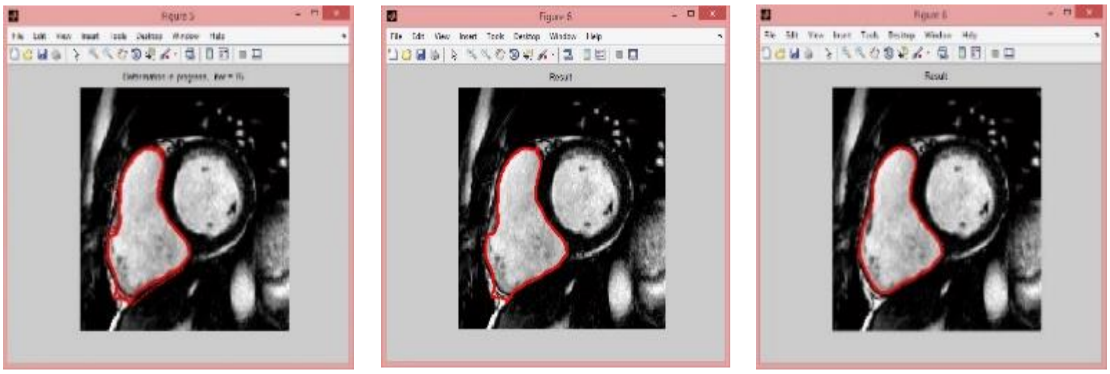

A B C

**Figure 8. ADF and GVF results based on Right Ventricle. (A) Initial Curves of GVF. (B) Result of GVF Model with $\mu = 1.05$ (C) Result of ADF with $\sigma = 0.9$ and $k = 0.04$**

and Fig. 8(b). However ADF active contours give an efficient and satisfactory output as shown in Fig. 7(c) and Fig. 8(c). The endocardium wall extraction has to deal with irregularities in the blood pool, noise and weak contours surrounded by strong ones. It can be clearly observed that the performance of ADF is more accurate and close to the manual segmentation than primitive GVF snake model as explained further.

### 4.4. Associated Manual and Semi-Automated Segmentation

Since the Manual segmentation of Cardiac MR Images by radiologist take an ample amount of time which include all slices per time frames, therefore the results of the proposed method show reliable segmentation and faster availability of segmented Cardiac MRI reports as shown in Fig 9.

 

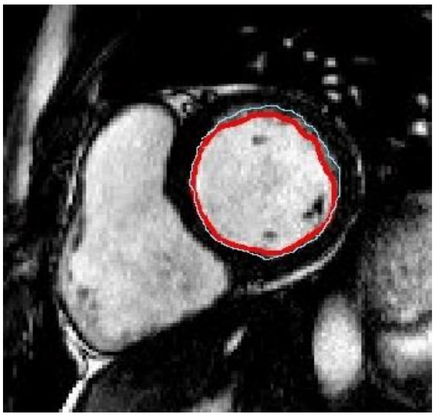

A

B

**Figure 9. Manual and Semi-Automated Segmentation. The Blue Color Thin Line is Manual Segmentation while the Red Bold Line Represents the ADF Semiautomatic Segmentation. (a) LV Endocardium Extraction (b) RV Endocardium Extraction**

### 4.5. Computation Time

All the examinations on cardiovascular MRI are completed in MATLAB 7.12.0.635 (R2011a), so the processing speed is computed by Central Processing Unit (CPU). The time taken for extracting the Endocardium layer from Cardiac MRI is calculated in seconds as shown in Table 1. All the three methods are were analyzed on the basis of computational time taken. Hence it is proved that ADF takes the minimum time for the extraction of endocardium tissue in both the ventricles. Moreover ADF takes 75 iterations to reach its final result which is less than GVF snake model [14].

Fig. 10 shows the time consuming plot in between GVF, ADF and Manual segmentation as per the frames, in one cardiac cycle there are 27 frames or slices from which 6 have been taken for plotting the graph. The red color shows that ADF active contours take minimum time and hence the computational cost will be less. Whereas the other two cases shown in blue and green indicates GVF and Manual segmentation methods respectively which show unevenness between consecutive frames and complexity of computational time and hence more expense.

 

**Table 1. Processing Time taken by GVF, ADF AND Manual Segmentation**

| MRI Frames | COMPUTATION TIME (IN SECONDS) | | | |
|---|---|---|---|---|
| | *Size* | *GVF* | *ADF* | *Manual* |
| 1 | 128×128 | 2.597 | 2.345 | 34.092 |
| 2 | 128×128 | 2.762 | 2.437 | 36.891 |
| 3 | 128×128 | 2.743 | 2.516 | 41.283 |
| 4 | 128×128 | 2.618 | 2.418 | 39.753 |
| 5 | 128×128 | 2.809 | 2.291 | 32.610 |
| 6 | 128×128 | 2.893 | 2.698 | 43.989 |

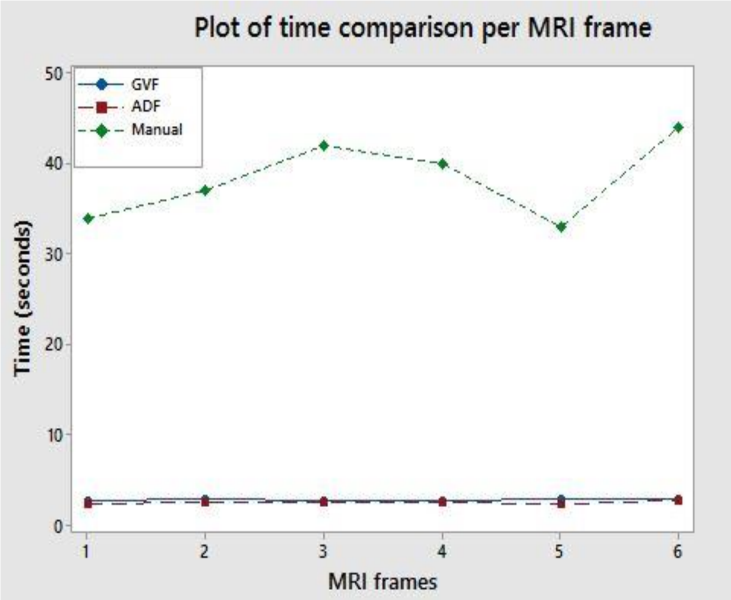


**Figure 10. Graphical Analysis Time vs. MRI Frames**

Further, the graphical analysis is based on the number of iterations and the curve evolution time in-between GVF and ADF is shown in Fig. 11. The GVF external forces take 200 iterations to reach segmented result of endocardium tissue in left ventricle for the evolution of curve in 2.893seconds while as ADF external forces take 75 iterations to complete the endocardium tissue extraction of left ventricle in 2.291 seconds. The graph shows less no of iterations performed by ADF active contours in less time as compared to that of GVF segmentation method and is an efficient method for carrying out the results than that of clinical methods.

 

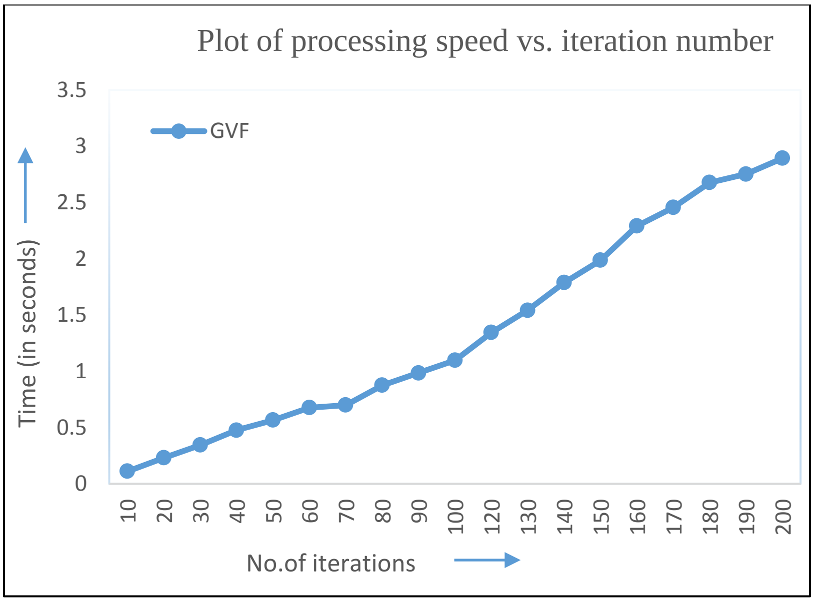


A

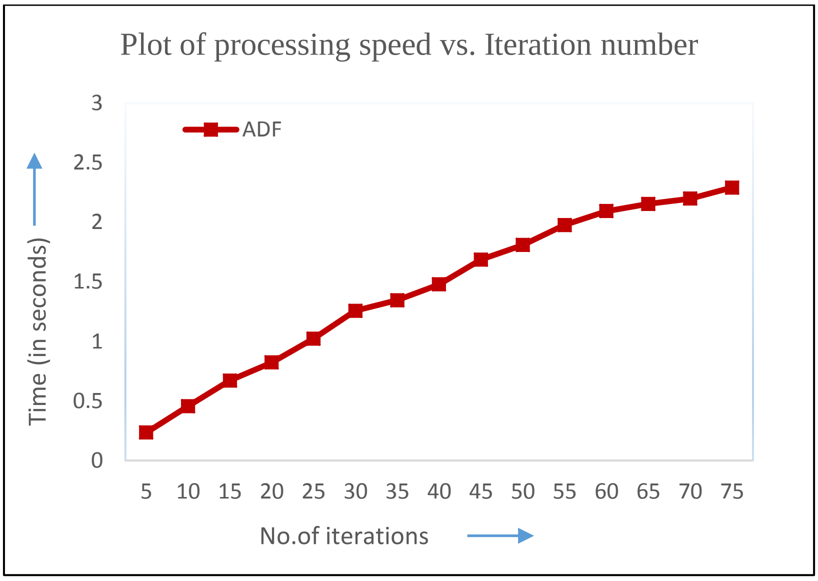


B

**Figure 11. Optimal Iteration Number with Processing C.P.U Time and Evolution of Curve (A) GVF (B) ADF**

## 5. Conclusion

This paper gives us a semiautomatic approach for extracting and segmenting the endocardium tissue from Cardiac MRI successfully. ADF model is based on hyper-surface harmonic minimal and infinite Laplace functional analysis which makes it a superior alternative for endocardium segmentation than traditional GVF. Its adaptive diffusion flow makes it movable according to the characteristics of loaded image regions. Experimental analysis on real Cardiac MR Images showed that GVF is a specific case of ADF in terms of large capture area and initialization insensitivity. In addition, ADF snakes are easily customized, take less processing time, prevent weak edges, less costly to implement in clinical diagnosis of cardiac function and are robust to noisy cardiac images. We have shown that the results based on proposed model show the availability of reliable and fast segmentation of left and right ventricle as compared to GVF external forces. The future extension to our work is to segment pericardium tissue of both left and right ventricle at the same instance in whole cascaded cardiac cycle.

## References

[1] A. Bhan, Y. Amin and R. Sreemathy, "Endocardium wall Extraction from noisy cardiac MR Images using modified Gradient Vector Flow Algorithm" IEEE conference on Medical imaging, m-health and communication systems (MedCom), **(2014)**, pp. 348-351.
[2] M. Kass, A. Witkin, and D. Terzopoulos, "Snakes-active contour models," International Journal of Computer Vision, vol. 1, **(1987)**, pp. 321–331.
[3] D. Terzopoulos, A. Witkin, and M. Kass,"Constraints on deformable models-recovering 3D shape and nonrigid motion,"Artif. Intell., vol.36, pp. 91–123, 1988.
[4] Y. Wu, Y. Wang and Y. Jia, "Adaptive diffusion flow active contours", International Journal of Computer Vision, **(2013)**, pp. 1421–1435.
[5] Bing Li and Scott T. Acton, Active Contour External Force Using Vector Field Convolution for Image Segmentation, IEEE transactions on image processing, vol. 16, **(2007)**, pp. 2096-2196.
[6] N. Paragios, R. Deriche, "Geodesic active regions and level set methods formotion estimation and tracking", Computer Vision and Image Understanding, vol. 97, no. 3, **(2005)**, pp. 259–282.
[7] D. Cremers, "Dynamical statistical shape priors for level set-based tracking", IEEE Transactions on Pattern Analysis and Machine Intelligence, vol. 28, no. 8, **(2006)**, pp. 1262–1273.
[8] T. Zhang, D. Freedman, "Tracking objects using density matching and shape priors", Proceedings of the Ninth IEEE International Conference on Computer Vision, 2003, IEEE, **(2008)**, pp. 1056–1062.
[9] A. Jalba, M. Wilkinson, J. Roerdink, CPM: a deformable model for shape recovery and segmentation based on charged particles, IEEE Transactions on Pattern Analysis and Machine Intelligence, vol. 26, no. 10, **(2004)**, pp. 1320–1335.
[10] L. Cohen, "On active contour models and balloons", CVGIP: Image Understanding, vol. 53, no. 2, **(1991)**, pp. 211–218.
[11] C. Xu, J. Prince, Snakes, shapes, and gradient vector flow, IEEE Transactions on Image Processing, vol. 7, no. 3, **(1998)**, pp. 359–369.
[12] V. Caselles, R. Kimmel, G. Sapiro, "Geodesic Active Contours", International Journal of Computer Vision, vol. 22, no. 1, **(1997)**, pp. 61-79.
[13] S. Ranganath, "Contour Extraction from Cardiac MRI studies using Snakes", IEEE Trans. on Medical Imaging, vol. 14, no. 2, **(1995)**.
[14] A. Bhan, "Parametric Models for segmentation of cardiac MRI with geometrical interpretation", IEEE conference on Signal Processing and Intergrated Networks, vol.1, **(2014)**, pp. 711-716.
[15] L. Rudin, S. Osher, E. Fatemi, Nonlinear total variation based noise removal algorithms, Physica D: Nonlinear Phenomena, vol. 60, no. 1–4, **(1992)**, pp. 259–268.
[16] T. Kohlberger, D. Cremers, M. Rousson, R. Ramaraj, and G. Funka-Lea, "4D shape priors for a level set segmentation of the left myocardium in SPECT sequences", MICCAI, **(2006)**, pp. 92–100.
[17] M.P. Jolly, "Combining edge, region, and shape information to segment the left ventricle in cardiac MR images", MICCAI, 2001, pp. 482–490.
[18] Y. Boykov, O. Veksler, and R. Zabih, "Fast approximate energy minimization via graph cuts", ICCV, **(1999)**, pp. 377–384.
[19] X. Lin, B. Cowan, and A. Young, "Model-based graph cut method for segmentation of the left ventricle", **(2005)**, pp. 3058–3062.
[20] M. Black, G. Sapiro, D. Marimont, D. Heeger, "Robust anisotropic diffusion", IEEE Transactions on Image Processing, vol. 7, no. 3, **(2002)**, pp. 421–432.
[21] C. Xu, J. Prince, "Generalized gradient vector flow external forces for active contours", Signal Processing, vol. 71, no. 2, **(1998)**, pp.131–139.
[22] R. Zabih, "Segmentation of the left ventricle in cardiac MR images using graph cut s with parametric shape priors", IEEE International Conference on Acoustics Speech and Signal Processing, **(2008)**, pp. 521-524.

## Authors

**Yabrin Amin**, She is in the Electronics and communication Engineer, Department. ASET, Amity University, Noida, U.P, India, 201313. yabrin7483@gmail.com

**Shoaib Amin Banday**, He received his B.TECH degree in Electronics and Communications Engineering from Islamic University of Science and Technology, J&K, India in year 2011. He has done his M. Tech. degree in Communication and Information Technology from National Institute of Technology, Srinagar, India in 2013. Presently he is a research scholar at NIT Srinagar in Department Of Electronics and Communication. His research interests are Image Processing, Pattern Recognition and Biometric Security.

**Ajaz Hussain Mir**, He has done his B.E in Electrical Engineering with specialization in Electronics & Communication Engineering (ECE) .He did his M.Tech in Computer Technology and Ph.D both from IIT Delhi in the year 1989 and 1996 respectively. He is Chief Investigator of Ministry of Communication and Information Technology, Govt. of India project: Information Security Education and Awareness (ISEA). He has been guiding PhD and M.Tech thesis in Security and other related areas and has a number of International publications to his credit. Presently he is working as Professor in the Department of Electronics & Communication Engineering at NIT Srinagar, India. His areas of interest are Biometrics, Image processing, Security, Wireless Communication and Networks.

 